

## SMALL-ANGLE X-RAY SCATTERING SPECTRA OF IRON-BASED MAGNETIC FLUIDS

### MALOKOTNO SIPANJE RENTGENSKEGA SPEKTRA MAGNETNIH TEKOČIN NA OSNOVI ŽELEZA

**Supagorn Rugmai<sup>1</sup>, Chitnarong Sirisathitkul<sup>2</sup>, Komkrich Chokprasombat<sup>2</sup>,  
Prawet Rangsa<sup>2</sup>, Phimphaka Harding<sup>2</sup>, Toemsak Sriksirin<sup>3</sup>, Pongsakorn Jantaratana<sup>4</sup>**

<sup>1</sup>School of Physics, Institute of Science, Suranaree University of Technology and Synchrotron Light Research Institute (Public Organization), Nakhon Ratchasima, Thailand

<sup>2</sup>Molecular Technology Research Unit, School of Science, Walailak University, Nakhon Si Thammarat, Thailand

<sup>3</sup>Department of Physics, Faculty of Science, Mahidol University, Bangkok, Thailand

<sup>4</sup>Department of Physics, Faculty of Science, Kasetsart University, Bangkok, Thailand  
schitnar@wu.ac.th

*Prejem rokopisa – received: 2011-11-29; sprejem za objavo – accepted for publication: 2012-03-05*

Two types of superparamagnetic nanoparticles, namely magnetite ( $\text{Fe}_3\text{O}_4$ ) and iron-platinum (FePt), with their surface modified by oleic acid and oleylamine were synthesized using the polyol process and dispersed in *n*-hexane. Vibrating-sample magnetometry (VSM) was used to characterize the FePt and the magnetic susceptibility of the  $\text{Fe}_3\text{O}_4$  was measured as a function of magnetic field and frequency at room temperature. Synchrotron, small-angle, X-ray scattering (SAXS) patterns revealed the polydispersity of the magnetic nanoparticles with average radii below 5 nm. As confirmed by transmission electron microscopy (TEM) images and dynamic light scattering (DLS), the  $\text{Fe}_3\text{O}_4$  nanoparticles had a larger average size. The DLS measurement gave larger radii than those obtained from the SAXS because of the effect of aggregates and surfactants.

Keywords: magnetic fluid, magnetite, iron-platinum, synchrotron radiation, SAXS

Dve vrsti superparamagnetnih nanodelcev, magnetit ( $\text{Fe}_3\text{O}_4$ ) in železo-platina (FePt), s površino, modificirano z oleinsko kislino in oleinaminom, sta bili sintetizirani s polyolnim postopkom in dispergirani v *n*-heksanu. Vibracijska magnetometrija vzorcev (VSM) je bila uporabljena za karakterizacijo FePt in magnetna občutljivost  $\text{Fe}_3\text{O}_4$  je bila izmerjena pri sobni temperaturi kot funkcija magnetnega polja in frekvence. Sinhrotronsko malokotno sipanje rentgenskih žarkov (SAXS) je odkrilo polidisperznost magnetnih nanodelcev s povprečnim premerom, manjšim od 5 nm. Kot so potrdili posnetki s transmisijsko elektronsko mikroskopijo (TEM) in dinamičnim sipanjem svetlobe (DLS), imajo nanodelci  $\text{Fe}_3\text{O}_4$  večjo povprečno velikost. Meritve DLS so pokazale večje premere delcev kot meritve SAXS zaradi učinka združevanja delcev in tenzidov.

Ključne besede: magnetna tekočina, magnetit, železo-platina, sinhrotronsko sevanje, SAXS

## 1 INTRODUCTION

Magnetic fluids are a special class of materials that possess the advantages of a liquid state of the carrier and a magnetic state of the nanoparticles.<sup>1</sup> Either ferromagnetic or superparamagnetic nanoparticles can be stabilized without agglomeration and sedimentation in a liquid by surfactant molecules, such as oleic acid and oleylamine.<sup>2</sup> In addition to an increase in the magnetization in response to an applied magnetic field, the single-domain, superparamagnetic particles are able to generate heat in an alternating magnetic field. Moreover, some product properties, such as magnetoviscosity, are exclusively observed in a magnetic fluid.<sup>1</sup> As a result, magnetic fluids are increasingly implemented in engineering and biomedical applications. Magnetite ( $\text{Fe}_3\text{O}_4$ ) nanoparticles in either water or oil are commercially available. In addition to the conventional uses, such magnetic fluids are the subjects of research and development as drug-delivery, hyperthermia and MRI-contrast agents.<sup>3,4</sup> On the other hand, iron-platinum (FePt) is investigated as a material for ultra-high-density recording.<sup>5</sup> The as-synthesized FePt nanoparticles in the

superparamagnetic state are commonly stored in the form of a magnetic fluid.

The magnetic properties of  $\text{Fe}_3\text{O}_4$  and FePt nanoparticles can be characterized in the forms of colloidal particles or dried particles on solid substrate using either a susceptometer or a magnetometer. Since their magnetic properties are highly dependent on the shape and size distribution, several techniques have been employed to characterize such nanoparticles. Transmission electron microscopy (TEM) provides images, but the qualitative analysis is based on sampling. Dynamic light scattering (DLS) gives an overall size distribution, but the size of the aggregate is usually measured instead of the individual particles.<sup>6</sup> Small-angle, X-ray scattering (SAXS) using a synchrotron source offers an alternative characterization of the shape and the size distribution. In addition to common uses in the case of organic nanostructures, the technique can also characterize magnetic nanoparticles, including ferrites<sup>7,8</sup>, maghemite<sup>9</sup>,  $\text{Fe}_3\text{O}_4$ <sup>6,10,11</sup> and FePt.<sup>12-14</sup>

In this work,  $\text{Fe}_3\text{O}_4$  and FePt nanoparticles synthesized using the polyol process and dispersed in hexane were characterized by synchrotron SAXS. The results

were used to complement those from DLS, TEM and magnetic measurements.

## 2 EXPERIMENTAL

The polyol processes adapted from Sun et al.<sup>15</sup> were carried out under standard airless Schlenk line techniques in a nitrogen ( $N_2$ ) atmosphere. For the  $Fe_3O_4$  nanoparticles, a mixture of 2.0 mmol of  $Fe(acac)_3$  (99.99 %), 10 mmol of 1,2 hexadecandiol (90 %), 6 mmol of oleic acid (90 %) and 6 mmol of oleylamine (70 %) was added to a 100-mL Schlenk flask containing 20 mL of benzyl ether (99 %). The solution was heated and dwelled at 200 °C for 2 h and then allowed to reflux at 300 °C for 30 min. In the synthesis of FePt, 1.0 mmol of  $Fe(acac)_3$  and 0.5 mmol of  $Pt(acac)_2$  (97 %) were poured into a flask, and then 20 mL of ethylene glycol was added. The mixture was moderately stirred, purged with  $N_2$  for 15 min at room temperature before increasing the temperature to 120 °C. After the addition of 5 mmol of oleic acid and 5 mmol of oleylamine, the solution was heated to 205 °C and then allowed to reflux for 2 h.

After the heating source was removed, the solution was allowed to cool down to room temperature under  $N_2$ . The product was precipitated by adding ethanol and separated by centrifugation. The precipitate was dispersed in *n*-hexane. Extra ethanol was added in this dispersion and the dispersion was centrifuged again for purification. After washing the particles in ethanol for three or more times, they were dispersed in *n*-hexane with the presence of a small amount ( $\approx 0.05$  mL) of oleic acid and oleylamine, followed by purging with  $N_2$  to remove the oxygen and then stored in glass bottles at 0–4 °C.

The morphology of the nanoparticles was inspected by TEM. The samples were prepared by depositing a few drops of the final hexane dispersion on a carbon-coated grid, acting as a substrate. Magnetization as a function of the applied magnetic field for the FePt nanoparticles was measured by vibrating-sample magnetometry (VSM). To characterize the magnetic properties of the  $Fe_3O_4$  nanoparticles, the mass susceptibility of the magnetic fluid in a capsule was measured as function of the static (dc) magnetic field, as well as alternating (ac) magnetic field and its frequency using a susceptometer at room temperature.

The SAXS measurements were performed at BL2.2 of the Synchrotron Light Research Institute, Thailand. The X-ray wavelength was set to 0.155 nm. A CCD detector (Mar SX165) was used to record the 2D scattering patterns. The sample-detector distance of 1587.46 mm, set for the experiments, was calibrated by measuring the scattering of silver behenate powder. For the measurements, each magnetic fluid was injected into a sample cell with aluminum foil windows. The background subtraction was carried out by subtracting the

sample scattering patterns from that of *n*-hexane. The absorptions of X-rays by the sample and the *n*-hexane were taken into account in the background-subtraction process by measuring the transmitted beam intensity, with reference to that of an empty cell, using a photodiode located in front of the beamstop. The scattering profiles for the FePt and  $Fe_3O_4$  nanoparticles were then obtained by circularly averaging the background-subtracted patterns.

## 3 RESULTS AND DISCUSSION

The variation of the complex magnetic susceptibility of the  $Fe_3O_4$  fluid with the frequency follows the trend previously shown by Fannin et al.<sup>16–18</sup> The response of the superparamagnetic fluid to an alternating magnetic field can be modeled and experimentally fitted. In **Figure 1a**, the real part is decreased gradually from  $1.6 \times 10^{-6}$  m<sup>3</sup>/kg at 100 Hz to  $1.4 \times 10^{-6}$  m<sup>3</sup>/kg at 600 Hz. It has a linear decrease with the log of the frequency from 800 Hz to 4 000 Hz before dropping to the saturation around  $4.0 \times 10^{-7}$  m<sup>3</sup>/kg at 6 000 Hz. The imaginary part is modest and remains constant over a wider frequency range from 100 to 1000 Hz. The peak in the literature<sup>16–18</sup> centered around 1500–2 000 Hz is not clearly observed. At a fixed frequency, the susceptibility does not have

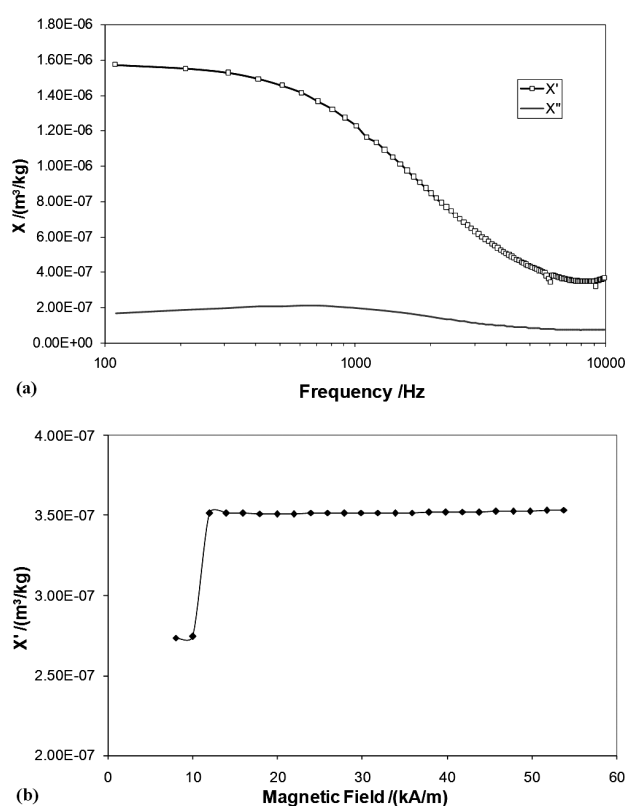


**Figure 1:** Susceptibility of  $Fe_3O_4$  in hexane as a function of: a) frequency and b) ac magnetic field at 7 kHz

**Slika 1:** Občutljivost  $Fe_3O_4$  v heksanu kot funkcija: a) frekvence in b) izmeničnega magnetnega polja pri 7 kHz

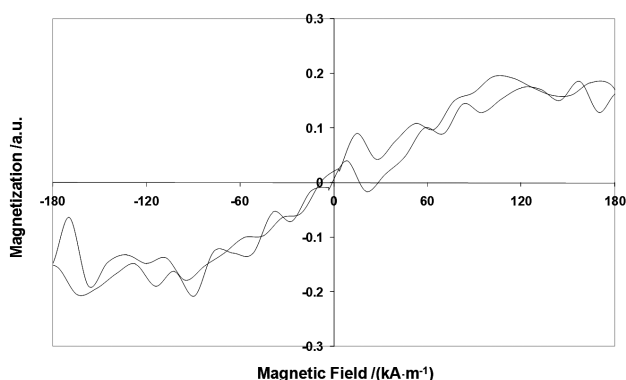


**Figure 2:** Magnetization of FePt as a function of applied magnetic field measured by VSM

**Slika 2:** Magnetizacija FePt kot funkcija uporabljenega magnetnega polja, izmerjena z VSM

significant variations in response to the changes in the dc magnetic field between  $-1$  kA/m and  $1$  kA/m and the ac magnetic field up to  $56$  kA/m. There is an exception in **Figure 1b**: the sudden increase in the real susceptibility from  $2.75 \times 10^{-7}$  to  $3.5 \times 10^{-7}$  m<sup>3</sup>/kg occurs by increasing the ac field from  $12$  kA/m to  $16$  kA/m. Similar behavior was previously observed in the case of maghemite.<sup>17, 18</sup> According to the magnetization curve in **Figure 2**, the FePt fluid also exhibits superparamagnetic behavior with saturation from  $180$  kA/m.

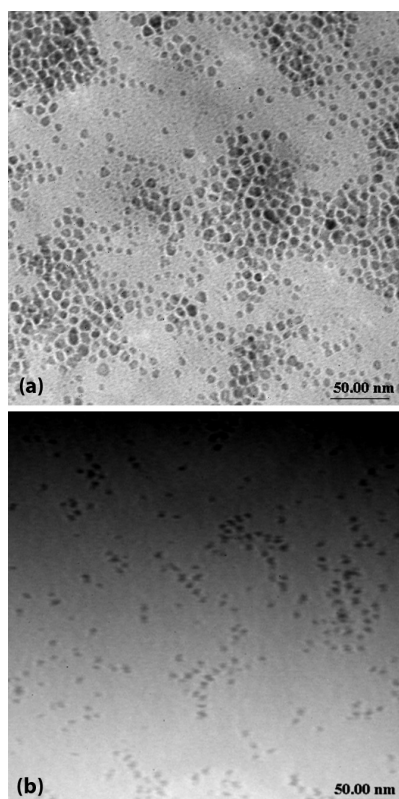


**Figure 3:** TEM images of: a) Fe<sub>3</sub>O<sub>4</sub> and b) FePt nanoparticles on substrates

**Slika 3:** TEM-posnetek: a) Fe<sub>3</sub>O<sub>4</sub>- in b) FePt-nanodelcev na podlagi

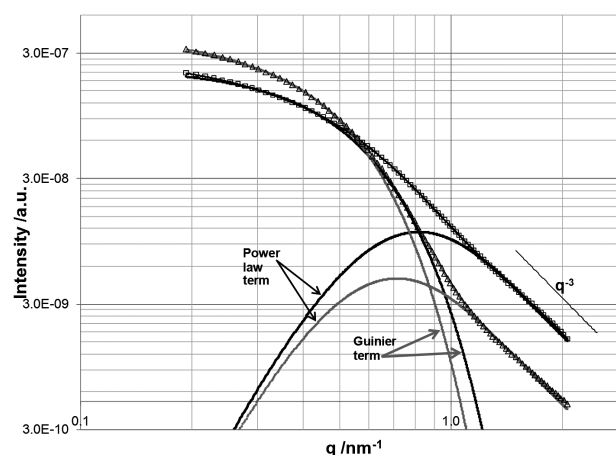


**Figure 4:** Measured SAXS profiles from FePt- (squares) and Fe<sub>3</sub>O<sub>4</sub>- (triangles) nanoparticles. The black and grey solid lines are the unified exponential power-law fits for FePt and Fe<sub>3</sub>O<sub>4</sub>, respectively, with the contributions from the Guinier and power-law terms. The  $q^{-3}$  line is shown to indicate  $-3$  slope obtained from the fit.

**Slika 4:** Izmerjen SAXS-profil iz FePt- (kvadrati) in Fe<sub>3</sub>O<sub>4</sub>- (trikotniki) nanodelcev. Črna in siva linija sta prilagojeni eksponentnemu zakonu za FePt in Fe<sub>3</sub>O<sub>4</sub>, združeni s prispevkom zakonitosti Guinierja in izrazi zakona moči. Prikazana je linija  $q^{-3}$ , ki kaže naklon  $-3$ , dobljen iz prilaganja.

TEM images of the as-synthesized particles are compared in **Figure 3**. The morphology of the Fe<sub>3</sub>O<sub>4</sub> nanoparticles can be described as spheroid with a rough surface. The size distribution around  $5$  nm in radius and some aggregates are observed. The FePt nanoparticles in **Figure 3b** are less concentrated and generally smaller than the Fe<sub>3</sub>O<sub>4</sub>. The DLS size distribution curves of surfactant-coated Fe<sub>3</sub>O<sub>4</sub> and FePt have their peaks centered at approximately  $7.96$  nm and  $4.28$  nm in radius, respectively.

The measured SAXS intensity profiles for FePt and Fe<sub>3</sub>O<sub>4</sub> are shown in **Figure 4**. The intensity profiles are plotted as a function of the scattering vector  $q$ , given by

$$q = 4\pi \sin\left(\frac{\theta}{\lambda}\right) \quad (1)$$

where  $\theta$  denotes half the scattering angle and  $\lambda$  is the X-ray wavelength. The measured SAXS intensity profiles from both the FePt and Fe<sub>3</sub>O<sub>4</sub> nanoparticles appear to have a certain slope in the high  $q$  region and then a transition to an exponential-like profile at small  $q$ . Considering the characteristics of the SAXS intensity profile of homogeneous spheres, the appearance of the measured intensity indicates that the  $q$ -range of the measurement may contain parts of the Guinier and the fractal regimes, as well as the transition between the two regimes.<sup>19</sup>

In order to analyze the particle size and size distribution, the unified exponential-power law model of Beaucage<sup>20</sup> was used to fit the measured data, where the scattering intensity is given by:

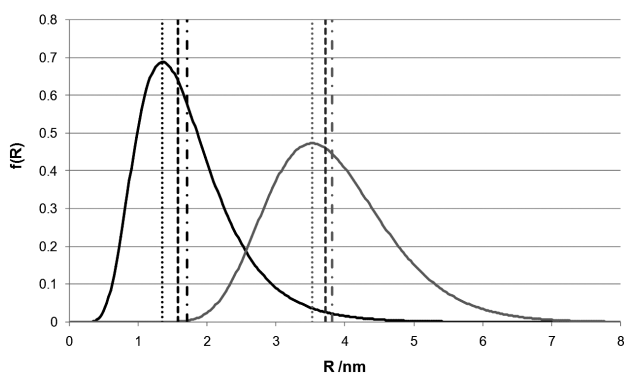


**Figure 5:** Lognormal size distributions for FePt (black solid line) and Fe<sub>3</sub>O<sub>4</sub> (grey solid line) obtained from the unified exponential power-law fit. The positions of the mode, median and mean radii are also shown for each distribution by dotted, dashed and dot-dashed lines, respectively.

**Slika 5:** Normalna logaritemska razporeditev velikosti FePt (črna linija) in Fe<sub>3</sub>O<sub>4</sub> (siva linija), dobljena iz poenotene eksponentne odvisnosti. Prikazane so tudi pozicije vrste srednje in največje velikosti delcev za vsako razvrstitev s pikčasto, črtkano in pikčasto-črtkano linijo.

$$I(q) = G \exp\left(-\frac{q^2 R_g^2}{3}\right) + B \left[ \left[ \operatorname{erf}\left(\frac{q R_g}{\sqrt{6}}\right) \right]^3 / q \right]^P \quad (2)$$

The prefactors  $G$  and  $B$ , the radius of gyration  $R_g$  and the exponent  $P$  are fit parameters. This model, including its more general form for multi-level structure,<sup>20</sup> has been successfully applied to describe systems with multiple structures.<sup>21–23</sup> The fitting was carried out with a least-squares minimization procedure using the software package SASfit.<sup>24</sup> The fitted scattering-intensity curves are shown in **Figure 4**, where contributions from the Guinier and the power law terms in Eq. (2) are also shown. The fitted exponent  $P = 3$  was obtained for both samples. This value is at the limit of the mass and surface fractal and may indicate contributions from a uniformly dense aggregate with a very rough surface.<sup>22</sup> To investigate the particle size and size distribution, the lognormal distribution of the particle size is assumed, where the lognormal distribution function is given by:<sup>25</sup>

$$f(R) = \frac{1}{R\sigma\sqrt{2\pi}} \exp\left\{-\frac{[\ln(R/m)]^2}{2\sigma^2}\right\} \quad (3)$$

with  $m$  denoting the median and  $\sigma$  is the shape parameter of the distribution. The mode, the value of  $R$  at the maximum, for the lognormal distribution is  $m \exp(-\sigma^2)$ . The mean particle radius  $\langle R \rangle$  can be found from the first moment of the distribution and is related to the two parameters of the distribution by:

$$\langle R \rangle = m \exp\left(\frac{\sigma^2}{2}\right) \quad (4)$$

where  $\langle R \rangle$  is the mean particle radius. The standard deviation ( $SD$ ) of the distribution is also related to the two parameters, and is given by:

$$SD = m \sqrt{\omega(\omega - 1)} \quad (5)$$

where  $\omega = \exp(\sigma^2)$ . Following Beaucage *et al.*,<sup>26</sup> the two parameters  $m$  and  $\sigma$  of the lognormal distribution can be explicitly given in terms of the ratio  $B/G$  and the radius of gyration  $R_g$  of the SAXS intensity profile. This enables one to extract the particle size and the distribution information from the fit of the unified model of Beaucage, Eq.(2), to the measured SAXS intensity profile. The parameters  $m$  and  $\sigma$  are given by:<sup>26</sup>

$$m = \sqrt{\frac{5R_g^2}{3 \exp(14\sigma^2)}} \quad (6)$$

$$\sigma = \sqrt{\frac{\ln(BR_g^4 / 1.62G)}{12}} \quad (7)$$

The value  $(BR_g^4 / 1.62G)$  in Eq.(7) also serves as an index of polydispersity, in which the value is 1 for a monodisperse sphere.<sup>20</sup> The lognormal distribution functions for both types of nanoparticles are shown in **Figure 5**. The relevant fitted parameters and calculated mean particle radii and standard deviations of the size distribution are shown in **Table 1**. The results give a smaller particle size for FePt than for Fe<sub>3</sub>O<sub>4</sub>, which agrees with the observation from the TEM images. The high standard deviation and index of polydispersity relative to the size of FePt can be described by the heterocoagulation model of FePt formation in the modified polyol process.<sup>27</sup> The obtained sizes of both types of particles are smaller than those obtained by DLS, which is a trend previously observed in the literature.<sup>6</sup> The reason is not only due to the exclusion of surfactants by the SAXS but also the effect of aggregation in the case of DLS.

**Table 1:** Fitted parameters for the SAXS intensity profile and calculated mean particle radius and standard deviation compared with the DLS results

**Tabela 1:** Prilagojeni parametri SAXS intenzitetnega profila in izračunan premer delca ter standardni odklon v primerjavi z DLS-rezultati

Sample	SAXS			DLS	
	$BR_g^4 / (1.62G)$	$R_g/\text{nm}$	$\langle R \rangle/\text{nm}$	$SD$	$R_{\text{peak}}/\text{nm}$
FePt	6.55	3.67	1.71	0.70	4.28
Fe <sub>3</sub> O <sub>4</sub>	1.92	4.21	3.82	0.90	7.96

## 4 CONCLUSION

Synchrotron SAXS spectra revealed the polydispersity of superparamagnetic Fe<sub>3</sub>O<sub>4</sub> and FePt nanoparticles in *n*-hexane synthesized using the polyol process. FePt nanoparticles had a smaller average size, which is in a good agreement with DLS and TEM images. The radii obtained from the DLS measurement tended to be larger than those from SAXS because the aggregates and surfactants were also taken into account.

## 5 REFERENCES

- <sup>1</sup> S. Odenbach, Recent progress in magnetic fluid research, *Journal of Physics: Condensed Matter*, 16 (2004) 32, R1135–R1150
- <sup>2</sup> A. Drmota, A. Kosak, A. Znidarzik, A mechanism for the adsorption of carboxylic acids onto the surface of magnetic nanoparticles, *Mater. Tehnol.*, 42 (2008) 2, 79–83
- <sup>3</sup> Q. A. Pankhurst, J. Connolly, S. K. Jones, J. Dobson, Applications of magnetic nanoparticles in biomedicine, *Journal of Physics D: Applied Physics*, 36 (2003) 13, R167–R181
- <sup>4</sup> S. Campelj, D. Makovec, L. Skrlep, M. Drogenik, Preparation of nano-composites for biomedical applications, *Mater. Tehnol.*, 42 (2008) 4, 179–182
- <sup>5</sup> S. Sun, Recent advances in chemical synthesis, self-assembly, and applications of FePt nanoparticles, *Advanced Materials*, 18 (2006) 4, 393–403
- <sup>6</sup> E. V. Shtykova, X. L. Huang, N. Remmes, D. Baxter, B. Stein, B. Dragnea, D. I. Svergun, L. M. Bronstein, Structure and properties of iron oxide nanoparticles encapsulated by phospholipids with poly(ethylene glycol) tails, *Journal of Physical Chemistry C*, 111 (2007) 49, 18078–18086
- <sup>7</sup> R. Itri, J. Depeyrot, F. A. Tourinho, M. H. Sousa, Nanoparticle chain-like formation in electrical double-layered magnetic fluids evidenced by small-angle X-ray scattering, *European Physical Journal E*, 4 (2001) 2, 201–208
- <sup>8</sup> F. L. O. Paula, G. J. da Silva, R. Aquino, J. Depeyrot, J. O. Fossum, K. D. Knudsen, G. Helgesen, F. A. Tourinho, Gravitational and magnetic separation in self-assembled clay-ferrofluid nanocomposites, *Brazilian Journal of Physics*, 39 (2009) 1A, 163–170
- <sup>9</sup> M. J. Park, J. Park, T. Hyeon, K. Char, Effect of interacting nanoparticles on the ordered morphology of block copolymer/nanoparticle mixtures, *Journal of Polymer Science Part B-Polymer Physics*, 44 (2006) 24, 3571–3579
- <sup>10</sup> N. Suzuki, P. Gupta, H. Sukegawa, K. Inomata, S. Inoue, Y. Yamachi, Aerosol-assisted synthesis of thiol-functionalized mesoporous silica spheres with Fe<sub>3</sub>O<sub>4</sub> nanoparticles, *Journal of Nanoscience and Nanotechnology*, 10 (2010) 10, 6612–6617
- <sup>11</sup> G. Utkan, F. Sayar, P. Batat, S. Ide, M. Kriechbaum, E. Piskin, Synthesis and characterization of nanomagnetite particles and their polymer coated forms, *Journal of Colloid and Interface Science*, 353 (2011) 2, 372–379
- <sup>12</sup> K. Shinoda, K. Sato, B. Jeyadevan, K. Tohji, S. Suzuki, Local structural studies of directly synthesized L10 FePt nanoparticles by using XRD, XAS and SAXS, *Journal of Magnetism and Magnetic Materials*, 310 (2007) 2, 2387–2389
- <sup>13</sup> C. Hendrich, L. Favre, D. N. Ievlev, A. N. Dobrynin, W. Bras, U. Hormann, E. Piscopiello, G. van Tendeloo, P. Lievens, K. Temst, *Applied Physics A*, 86 (2007) 4, 533–538
- <sup>14</sup> C. C. H. Lo, S. C. Tsang, C. H. Yu, K. Tam, Magnetic properties of macroscopic colloid crystals of silica-coated FePt nanoparticles with controllable interstices for molecular separation, *Journal of Applied Physics*, 105 (2009) 7, 07C101
- <sup>15</sup> S. Sun, H. Zeng, D. B. Robinson, S. Raoux, P. M. Rice, S. X. Wang, G. Li, Monodisperse MFe<sub>2</sub>O<sub>4</sub> (M = Fe, Co, Mn) nanoparticles, *Journal of the American Chemical Society*, 126 (2004) 1, 273–279
- <sup>16</sup> P. C. Fannin, Investigating magnetic fluids by means of complex susceptibility measurements, *Journal of Magnetism and Magnetic Materials*, 258–259 (2003), 446–451
- <sup>17</sup> P. C. Fannin, C. Mac Oireachtaigh, L. Cohen-Tannoudji, E. Bertrand, J. Bibette, Complex susceptibility measurements of a suspension of magnetic beads, *Journal of Magnetism and Magnetic Materials*, 300 (2006) 1, e210–e212
- <sup>18</sup> P. C. Fannin, L. Cohen-Tannoudji, E. Bertrand, A. T. Giannitsis, C. Mac Oireachtaigh, J. Bibette, Investigation of the complex susceptibility of magnetic beads containing maghemite nanoparticles, *Journal of Magnetism and Magnetic Materials*, 303 (2006) 1, 147–152
- <sup>19</sup> G. C. Bushell, Y. D. Yan, D. Woodfield, J. Raper, R. Amal, On techniques for the measurement of the mass fractal dimension of aggregates, *Advances in Colloid and Interface Science*, 95 (2002) 1, 1–50
- <sup>20</sup> G. Beaucage, Approximations leading to a unified exponential/power-law approach to small-angle scattering, *Journal of Applied Crystallography*, 28 (1995) 6, 717–728
- <sup>21</sup> G. Beaucage, D. W. Schaefer, Structural studies of complex systems using small-angle scattering: a unified Guinier/power-law approach, *Journal of Non-Crystalline Solids*, 172–174 (1994) 2, 797–805
- <sup>22</sup> D. W. Schaefer, R. S. Justice, How nano are nanocomposites?, *Macromolecules*, 40 (2007) 24, 8501–8517
- <sup>23</sup> G. J. Schneider, V. Vollnhals, K. Brandt, S. V. Roth, D. Goeritz, Correlation of mass fractal dimension and cluster size of silica in styrene butadiene rubber composites, *Journal of Chemical Physics*, 133 (2010) 9, 094902
- <sup>24</sup> J. Kohlbrecher: A program for fitting elementary structure models of small angle scattering data. Available from World Wide Web: <http://kur.web.psi.ch/sans1/SANSSoft/sasfit.html>
- <sup>25</sup> C. Forbes, M. Evans, N. Hastings, B. Peacock, *Statistical Distributions*, 4<sup>th</sup> ed., John Wiley and Sons Inc., New York 2011, 131
- <sup>26</sup> G. Beaucage, H. K. Kammler, S. E. Platsinis, Particle size distributions from small-angle scattering using global scattering functions, *Journal of Applied Crystallography*, 37 (2004) 4, 523–535
- <sup>27</sup> W. Beck Jr., C. G. S. Souza, T. L. Silva, M. Jafelicci Jr., L. C. Varanda, Formation mechanism via a heterocoagulation approach of FePt nanoparticles using the modified polyol process, *Journal of Physical Chemistry C*, 115 (2011) 21, 10475–10482